MNRAS 502, 6094-6100 (2021) Advance Access publication 2021 February 22



Downloaded from https://academic.oup.com/mnras/article/502/4/6094/6146086 by guest on 23 July 2021

## On the radio frequency dependence of the pulse delay phenomenon in PSR B0943 + 10

S. A. Suleymanova, 1 \* A. N. Kazantsev , 1 J. M. Rankin and S. V. Logvinenko 1

1P. N. Lebedev Physical Institute of the Russian Academy of Sciences, Pushchino Radio Astronomy Observatory, Pushchino 142290, Russia

Accepted 2021 February 11. Received 2021 February 11; in original form 2021 January 25

#### ABSTRACT

We report the result of measurements of a gradual shift of the integrated pulses towards later spin phase of the anomalous pulsar B0943+10 at high radio frequencies. We have used observations from the Arecibo Observatory and the GMRT at 327 and 325 MHz correspondingly. For the measurements, we have proposed a special method for calculating the correct positions of the partially merged two components of the pulse profile shape with significant temporal changes in their amplitude ratio. The exponential change in the pulse phase with an amplitude of 4 ms and characteristic time of about 1 h has been found. Comparison of our measurements at 325 and 327 MHz with those at the lower frequencies of 25-80, 62 and 112 MHz have shown that the character of the process does not depend on frequency across a wide frequency range. The result is very important for constraining the nature of the delay. It supports the assumption that the process results from changes in the vacuum gap near the surface of the pulsar. The further correlation between changes in the pulse phase and its intensity is discussed.

**Key words:** stars: neutron – pulsars: general – pulsars: individual: B0943+10 – pulsars: individual: J0946+0951.

### 1 INTRODUCTION

Radio pulsar B0943+10 is a well-studied exemplar of the modechanging pulsars. Such pulsars have two or more metastable states with distinct radio-emission properties. PSR B0943+10 was discovered in 1968 using the DKR-1000 cross radio telescope at Pushchino Radio Astronomy Observatory (PRAO) at 80 MHz (Vitkevich et al. 1969). Later observations in 1980 exhibited the contrasting characteristics of its dual modes at 62 MHz (Suleymanova & Izvekova 1984). The authors showed that the pulsar's emission switches within a single rotation between a quiet (Q mode) and a bright Burst (B mode) one. Subsequent investigations showed that PSR B0943+10 demonstrates additional remarkable behaviors: its B mode exhibits a highly regular and stable subpulse drift effect that prompted discovery that its subpulses are produced by a carousel beam system of 20 beamlets rotating through our sightline over some 37 pulses (Deshpande & Rankin 1999, 2001).

A further unusual property of the pulsar's modes is their long durations, and subsequent Arecibo investigations at 327 MHz identified continuous changes in the B-mode subpulse drift rate, averageprofile shape, and fractional linear polarization over durations of several hours (Rankin & Suleymanova 2006; Suleymanova & Rankin 2009) - and these later facilitated discovery of the two mode's different X-ray emissivities (Hermsen et al. 2013). The amplitude of the continuous subpulse drift rate variations is observed to be about 5 per cent. These variations correlate well with the B-mode variations in average pulse shape (and polarization), as represented by the peak amplitude ratio of two profile components: R = A2/A1.

The R-value decreases monotonically from 1.7 to 0.2 over a 4h interval following B-mode onset at 327 MHz. Studies of this phenomenon at lower frequencies, carried out in PRAO, have shown that the R-value is strongly frequency-dependent. The ratio varies in the range 1.2-0.2, 0.7-0.2, and 0.4-0.2 at 112, 62, and 42 MHz, respectively (Suleymanova & Rankin 2009).

In contrast, variations of the subpulse drift rate following B-mode onset demonstrate a different behaviour. Measurements at 327, 325, and 53 MHz (Rankin & Suleymanova 2006; Backus, Mitra & Rankin 2011; Bilous 2018) have shown that the amplitude and exponential decay time of the drift rate does not depend on frequency and indeed remains constant over decades. Based on these results, we can see that the pulsar's B-mode characteristics behave differently with frequency. To further investigate the magnetospheric processes during its B mode, we need to study the frequency dependence of a new feature in the radio emission of B0943+10-i.e. the systematic pulse displacement with B-mode age.

This phenomemon was discovered in 2014 (Suleymanova & Rodin) with PRAO's Large Phased Array (LPA) at 112 MHz using a pulse-timing analysis. Timing parameters were determined using the program TEMPO.<sup>1</sup> The LPA observations span 2007–2013 and comprise several hundred 3.5-min transits through the telescope beam. Standard timing analysis showed that residual deviations from the predicted times of arrival (TOA) correlate strongly with the Bmode profile shape. That is, profiles with larger R values arrived earlier. It was shown that the larger R values correspond to earlier ages or times from the B-mode onset (Rankin & Suleymanova 2006).

<sup>&</sup>lt;sup>2</sup>Physics Department, University of Vermont, Burlington, VT 05405, USA

It is worth noting that the average pulse results from integration of several hundred individual pulses.

<sup>\*</sup> E-mail: suleym@prao.ru

<sup>&</sup>lt;sup>1</sup>https://github.com/nanograv/tempo.

Hence, the conclusion was drawn that this systematic pulse displacement to later longitudes within the emission window is connected with the burst age. For values 1.0 > R > 0.2, the total pulse shift was found to be 4.6 ms. This effect was independently and somewhat later discovered using the LOFAR radio telescope in its 25-80 MHz low band (Bilous et al. 2014). Observations were carried out while tracking of the pulsar in its B mode over 4 h. The total displacement of the pulse midpoints were found to be nearly 4 ms as well. It was also shown that the pulse displacement rate decreases exponentially with time following B-mode onset. The phenomenon has been called 'pulse delay' (Bilous et al. 2014). However, this term is applicable only if the pulse longitude at B-mode onset is taken to be zero. When using a timing technique for pulse displacement measurements, the pulse position is measured as a residual deviation with the predicted TOA taken as  $t_0$ . According our measurements, the predicted TOA corresponds to B-mode age of about 1.4 h. In this case, the residuals for the first tens of minutes after B-onset have negative values, such that the profiles precede the predicted TOA.

The dependence of the TOA residual deviations on B-mode age, based on the large archives of PRAO observations at frequencies of 112 and 62 MHz was studied by Suleymanova & Pugachev (2017). For every B0943+10 profile, each reflecting a transit through the telescope beam, the TOA deviation and the B-mode age were calculated. The B-mode age of each transit encounter was determined from the subpulse drift rate, taking into account the behaviour of its time dependence (Rankin & Suleymanova 2006). From these, the exponential character of the longitudinal shift through the pulse window was confirmed. In addition, it was found that the negative deviations during the first minutes after B-mode onset typically fall in the -3 to -5 ms range for different observation sessions, which, in turn, correspond to total changes in pulse displacement of between 4 and 6 ms.

One can see that this pulse shift phenomenon was discovered and well investigated at PRAO at low frequencies of 112 and 62 MHz and using the LOFAR 25–80 MHz low band. Both investigations noted the absence of any discernible frequency dependence; however, perhaps this circumstance results merely from their similar low-frequency ranges.

In this paper, we present the results of measurements using the higher 327-MHz band. Our objective has been to investigate the 'pulse delay' phenomenon over a wider frequency range. We were able to use archival observations recorded using Arecibo in 2003 and the Giant Metrewave Radio Telescope (GMRT) in 2010 (Backus et al. 2011), and a further set associated with a simultaneous radio/X-ray campaign (Mereghetti et al. 2016) in 2014.

### 2 OBSERVATIONS AND METHODS

For a beginning, we used the Arecibo 327-MHz observations carried out in 2003 and 2014. Pulse phase resolution for 2003 is 0:35, and that for 2014 1:4. Luckily, the observations on MJD 52709, MJD 52916, and MJD 52832 include the instant of switching from the Q to B mode. In spite of the fact that the tracking time with Arecibo for PSR B0943+10 is about 2 h, the recorded durations of the B-mode apparitions after their onsets is 77, 71, and 42 min, respectively. In the three other 2003 observations sessions, the records contains pure B mode (MJD 52711, 52840, and 52917). These six observations also provided the basis of our earlier (Rankin & Suleymanova 2006) study.

Four of the 2014 runs (MJD 56964, 56966, 56984, and 56986) also represent pure B-mode intervals.

These Arecibo 327-MHz observations contains up to some 7000 individual pulses. This allows the full sequences to be divided into subaverages, each with a duration of 4.7 min and comprising 256

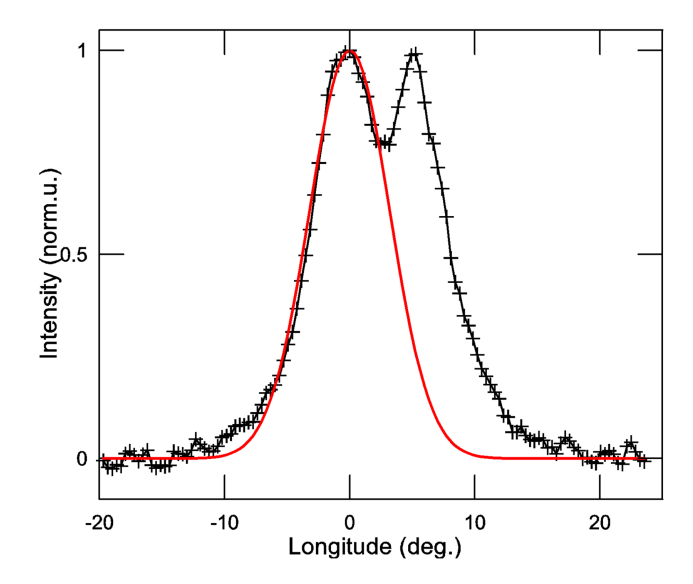


**Figure 1.** PSR B0943+10 partial profile (MJD 52709) obtained by averaging individual pulses during the initial 19 min following the B-mode onset (line with crosses). The solid (red) line shows a Gaussian with a standard deviation of 3°, which approximates the first component of the profile.

individual pulses. These subaverage pulse profiles provided the data for our pulse-profile timing analysis below.

As noted in our earlier investigations (Suleymanova & Rodin 2014; Suleymanova & Pugachev 2017), the longitude-axis position of the average pulse profile can be determined most reliably by measurements of the well-resolved first component. Owing to its brightness and shape, it can be taken as a template at low frequencies. The times of arrival of pulses for a given day of observations were determined by measuring the weighted centre of the cross-correlation function of the current profile and a template. The current average profile was the result of accumulating signal over the duration of the pulsar's transit: 15 min with the DKR-1000 at 62 MHz and 3.5 min for the LPA at 112 MHz.

This technique cannot be applied at higher frequencies. The two components of the B-mode pulse profile are partially merged at 327 MHz, so in order to distinguish them, we fitted two Gaussian functions to pulse profile. The widths of the Gaussians and the distance between them at 327 MHz were determined beforehand and found to remain constant.

### 2.1 The Gaussian parameters

Our earlier studies resolved the two components of the average B-mode 62- and 112-MHz profiles of PSR B0943+10 and showed that the widths of the first and second components are equal. This conclusion is in accordance with measurements at frequencies below 80 MHz at LOFAR (Bilous et al. 2014). We can reasonably assume that they are equal at higher frequencies as well, and therefore the average pulse profiles there can be described by two Gaussians of equal width. To determine the width of the Gaussian, we used a profile from the first 19 min after the B-mode onset (MJD 52709), where there was a marked saddle between the two components. In Fig. 1, this profile is shown by a line with crosses. The shape of the trailing wing of the first component of the pulse profile echoes the shape of its leading wing. As a result, the Gaussian representing the profiles's first component at 327 MHz has a standard deviation of 3.0, which corresponds to a full width at half-maximum width of

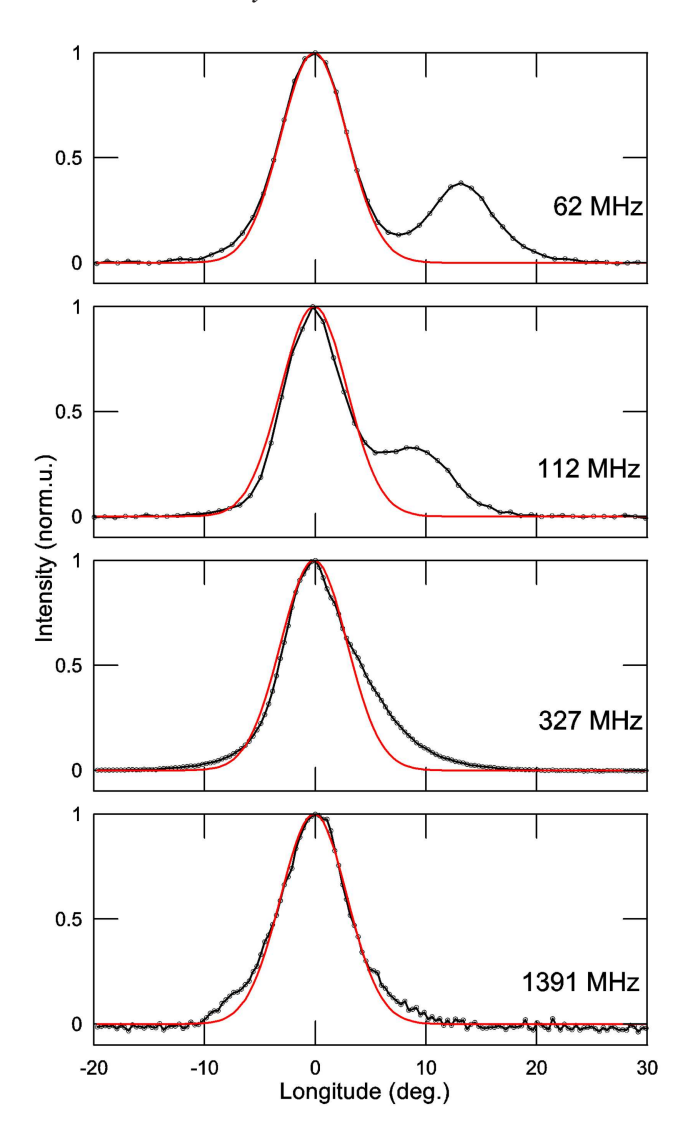


**Figure 2.** PSR B0943+10 average profiles at frequencies in the 62–1391 MHz range (black). The thin (red) line represents a Gaussian function with a 3° standard deviation. Comparison shows that the width of the first component remains nearly constant over a wide frequency range, in contrast to the strongly varying distance between the two components.

2.355 rms = 7.1, or 21.5 ms. This profile was used as a template for out further analyses.

Comparison of this template with the first components of average profiles at other frequencies shows its near constant width. Fig. 2 shows typical B0943+10 profiles at frequencies between 62 and 1391 MHz. The latter profile at 1391 MHz was obtained using Arecibo in 2012 (MJD = 55937; 0.35 resolution) and is presented here for the first time. This profile corresponds to the final stage of pulse-shape evolution just before transition back to the Q mode and hence is almost uninfluenced by its second component. The thin red lines represents the template with an rms =  $3^{\circ}$ . The comparison demonstrates that over this wide frequency range the first component's width does not change appreciably, in contrast to the dramatic increasing distance between the two components with wavelength. A question here might be the effect of dispersion smearing of the profile at these low frequencies. The observations were conducted using a digital receiver with 512 channels of 4.88kHz width and time resolution 2.87 ms. At 62 and 112 MHz, the

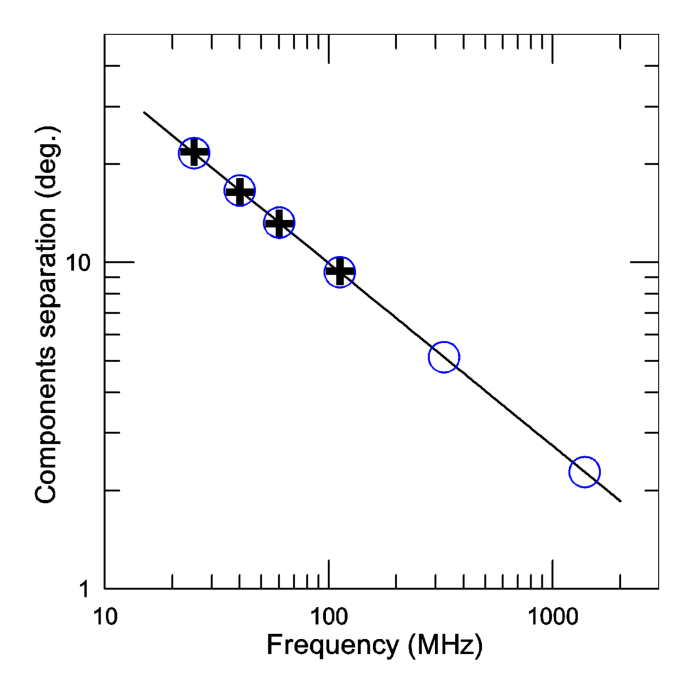


**Figure 3.** Frequency dependence of the distance *s* between the average-profile components of PSR B0943+10 in the 25-1391–MHz range. This separation is well described by a power law with an index of  $-0.56 \pm 0.07$ . The measurements were carried out at frequencies of 25, 40, 62, and 112 MHz (crosses). Extrapolating the function to 325/327 MHz gives values of  $5.15/5.12^{\circ}$  as well as just over  $2^{\circ}$  at 1.4 GHz (circles).

total time shift of a pulse within a single channel for a dispersion measure of  $15.4~\rm pc~cm^{-3}$  is  $2.7~\rm ms$  and  $0.47~\rm ms$  or  $0.9~\rm and~0.15$ , respectively; so the effects of instrumental broadening of the profiles can be neglected.

### 2.2 Distance between components

In order to accurately determine the positions (rotational phase) of the Gaussian-modelled average profile components, it is necessary to know the distance between them. Note that the pulsar's rotational period (P1) of 1.097 sec corresponds to 360° of longitude. The separation between the two components (distance between the peaks of the fitted Gaussians), s, was determined by studying its lowfrequency dependence. Fig. 3 plots this component separation within the average profiles of B0943+10. Measurements at frequencies of 40, 62, and 112 MHz were carried out with profiles from the DKR-1000 and LPA telescopes of PRAO. The 25-MHz measurement is taken from an Arecibo observation (Phillips & Wolszczan 1989). In the frequency range between 25 and 112 MHz, the component separation closely follows a power law with an index of  $-0.56 \pm 0.07$ . This value nearly coincides with the  $-0.57 \pm 0.01$  value that was obtained in the LOFAR low band range of 25-80 MHz (Bilous et al. 2014). According to the dependence  $s=130^{\circ}.8 \times f_{\rm MHz}^{-0.56}$ , the s values are 21°.6, 16°.6, 13°.2, and 9°.3 at frequencies 25, 40, 62, and 112 MHz, respectively. Extrapolating the function to 325/327 MHz gives a value of 5°.1.

# 2.3 Time dependence of the average-profile component amplitude ratio

In order to check the validity of the two-Gaussian model of the average profile when the its components are closely separated, we

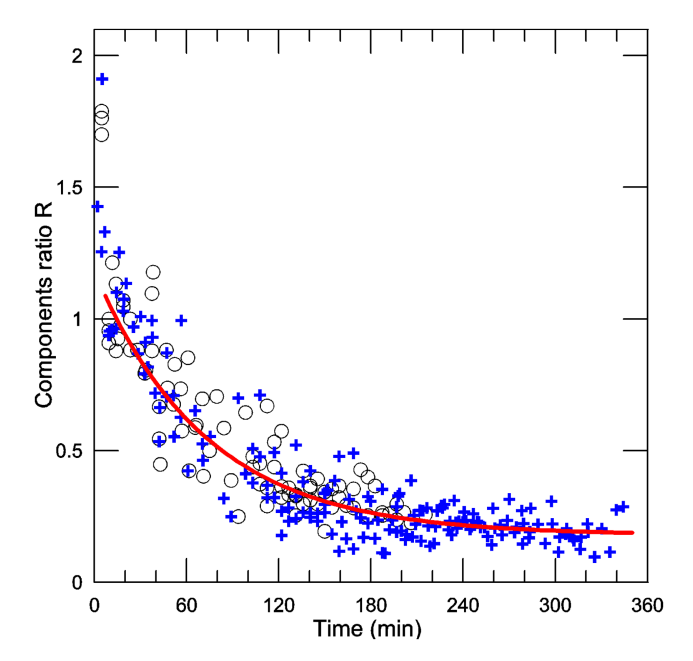


**Figure 4.** Gradual changes in PSR B0943+10's average profile shape as a function of time after the B-mode onset at 327 MHz (crosses). The amplitude ratio of the two component peaks R = A2/A1 is obtained by the Gaussian fitting procedure. For B-mode age from 7 to 344 min, the component-amplitude ratio varies from 1.2 to 0.2 according to the relation:  $R = 0.18 + \exp(-t/73 \text{ min})$ . The values published previously for the first 215 min after B-mode onset at 327 MHz (Rankin & Suleymanova 2006) are shown for comparison (circles).

compare our results with those (Rankin & Suleymanova 2006) published earlier using the same observations. Fig. 4 plots the component-peak ratio R in this work (circles) together with those stemming from the model. Initially, only the 2003 observations were used: MJD 52709, 52916, 52832, 52711, 52840, and 52917. Days 52709, 52916, and 52832 encounter a mode switch, and hence the starting moment  $t_0$  of the B-mode onset is known. For the other pure B-mode days, the B-mode age was determined in the above work and corresponds to 84, 112, and 103 min, respectively.

Fig. 4 also plots the Arecibo 2014 component ratios (MJD 56964, 56966, 56984, and 56986). These days do not include a B-mode transition, so the B-mode age was determined using the relation:  $R = 0.17 + 1.16 \exp(-t/73.3 \min)$  (Rankin & Suleymanova 2006), where R is equal to its average value for a given day. For the average R values of 0.242, 0.194, 0.220, and 0.211, the initial B-mode age of each sequence was determined to be 151, 278, 197, and 199 min, respectively. As a result, the interval over which the R dependence can now traced has increased from 215 (3.5 h) to 344 min (5.7 h). Fig. 4 shows that for times between 7 and 344 min, the ratio of the component-amplitude ratios decrease monotonically from 1.1 to 0.2 according to the revised relationship:  $R = 0.18 + \exp(-t / 73 \text{ min})$ . The coincidence of these two expressions for the time dependence of R demonstrates that our method of fitting B-mode profiles with two Gaussians of established widths and separations adequately measures the component amplitudes that can then be used to determine their positions on the longitude axis as well as their B-mode ages.

# 3 DETERMINATION OF THE AVERAGE-PROFILE SHIFT

In order to provide a stronger analysis of the average-profile time shifts, we also analysed a long (8-h) 325-MHz GMRT observation.

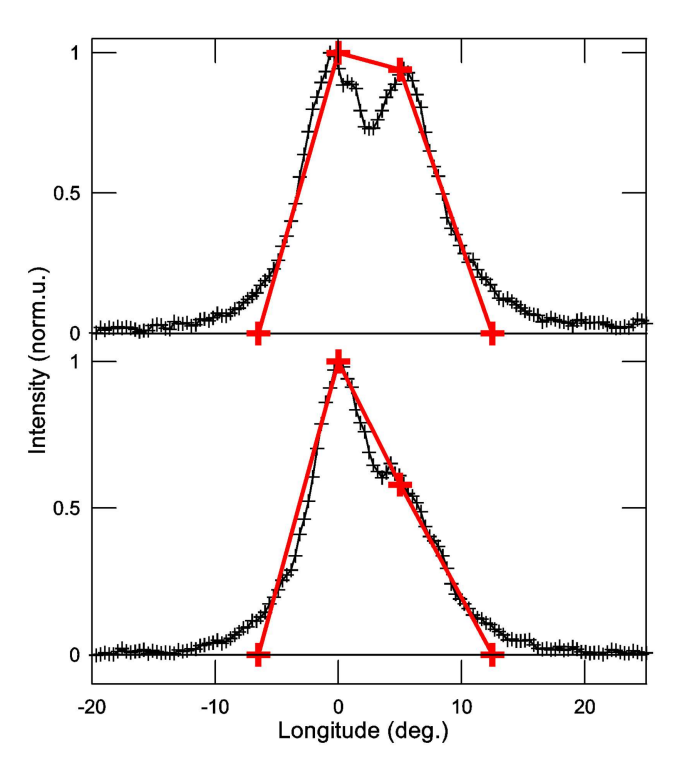


**Figure 5.** Average pulse profiles (MJD 52916) with R=0.94 and 0.58 corresponding to B-mode ages of 9 and 70 min, respectively, are shown (crosses). The quadrangles with bottoms and tops of 19° and 5°, respectively, simulate actual profiles with the same ratio of peaks.

This unique observation made in 2010 January (MJD 55210) was discussed in detail in Backus et al. (2011). This important observation allows us to follow variations in the pulse phase over 5.5 h. Overall, it consists of 23 000 pulses that include a transition from the Q to B mode. The B-mode portion of 18 000 pulses (with the time resolution of 0.512 ms) was divided on to 500-pulse subaverages. This GMRT 325-MHz observation practically coincides within its band limits with our Arecibo 327-MHz one; therefore, all of the above profile-structure estimates for 327 MHz are applicable to the 325-MHz sequence.

As was discussed above B0943+10's average-pulse components at 325 and 327 MHz are partially merged. In addition, during the evolution of the B mode, the ratio of their amplitudes R changes by almost an order of magnitude. In this situation, the direct determination of the position of the components by the method of fitting profiles with two Gaussians may not be perfectly correct. The position of the pulse may well shift from the middle position depending on the degree of dominance of the first or the second component. To determine the extent of this effect, we performed the following simulation: a quadrangle with a bottom and top sides equal to 19° and 5°, respectively, was chosen as a profile model. The top side is the horizontal distance between two upper quadrangle vertices, with these parameters the width of the model is equal to the actual profile width at the 0.5 amplitude level. The upper side of the figure corresponds to the distance between the components at a frequency of 327 MHz. The height of the front side of the quadrangle at a longitude of 0 degrees is constant and equal to 1, and the height of the side at a longitude of  $5^{\circ}$  varies from 2 to 0 with a step of 0.1.

Fig. 5 shows average profiles corresponding to different B-mode ages, and therefore, having different component-amplitude ratios. The actual profiles are taken from our 2003 (MJD 52916)

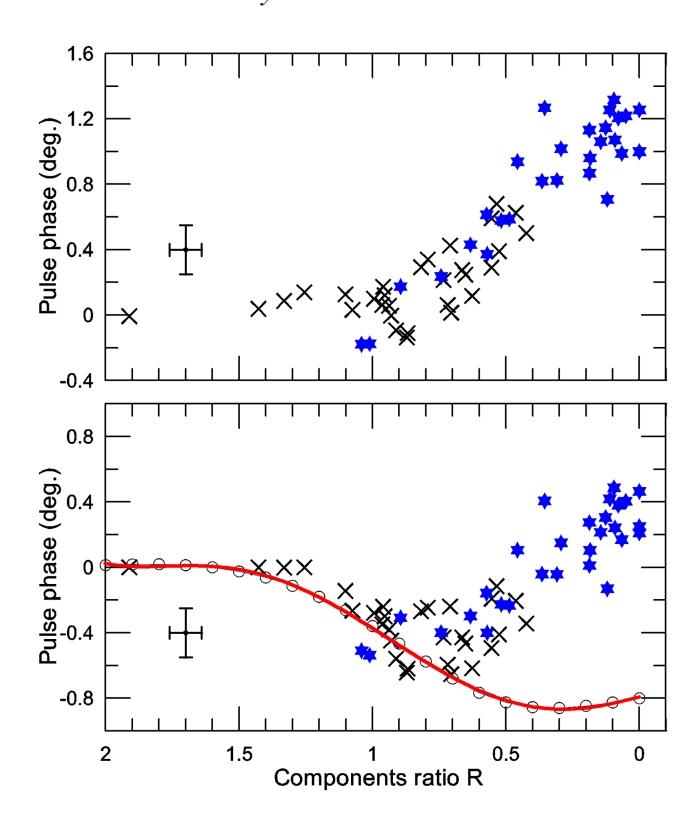


Figure 6. Lower panel: pulse phase as a function of the component-peak ratio measured by fitting two Gaussians to average profiles at 327 MHz (crosses), at 325 MHz (asterisks), and of simulated profiles (circles). The displacements of the simulated profiles are well described by a fifth-degree polynomial (solid red line). The zero value of the function corresponds to the profile at the moment of B-mode onset with  $R \ge 1.5$ . The B-mode age grows to the right. Upper panel: the same dependence relative to the fitted fifth-degree polynomial function.

observation. Profiles with R = 0.94 and 0.58 correspond to B-mode ages of 9 and 70 min, respectively. As a first approximation, the simulated profiles describe rather well the shape of the actual ones with a variable ratio of component amplitudes. The result of fitting simulated profiles with two Gaussians is shown in Fig. 6 (low panel, circles). The shift in the position of the pulse is well described by a fifth-degree polynomial (solid line):

$$Y = 0.40X^5 - 1.78X^4 + 2.15X^3 + 0.08X^2 - 0.42X - 0.79,$$
 (1)

The zero value of the function corresponds to the position of the pulse in the vicinity of the B-mode onset, where the second component dominates,  $R \ge 1.5$ . Subsequently, with a decreasing relative amplitude of the second component, the measured position of the pulse is increasingly influenced by the relatively brighter leading component - that is, it shifts to negative longitude values. For the simulated pulse profiles in the absence of additional factors affecting the position of the pulse, the total shift in longitude of the entire pulse and its components is of about -0.8 or -2.4 ms. This value is correct for rms  $= 3^{\circ}$  and depends on the width of Gaussian. Note that when two Gaussians with fixed widths and spacing were used in the fitting procedure, then the position changes of the first component reflect the position of the entire profile.

The dependence of the actual profile phase as a function of peak ratio is shown in Fig. 6 (lower panel) with crosses indicating Arecibo 327 MHz and asterisks GMRT 325 MHz. Generally, these measured phase values should suffer the influences of two effects acting in

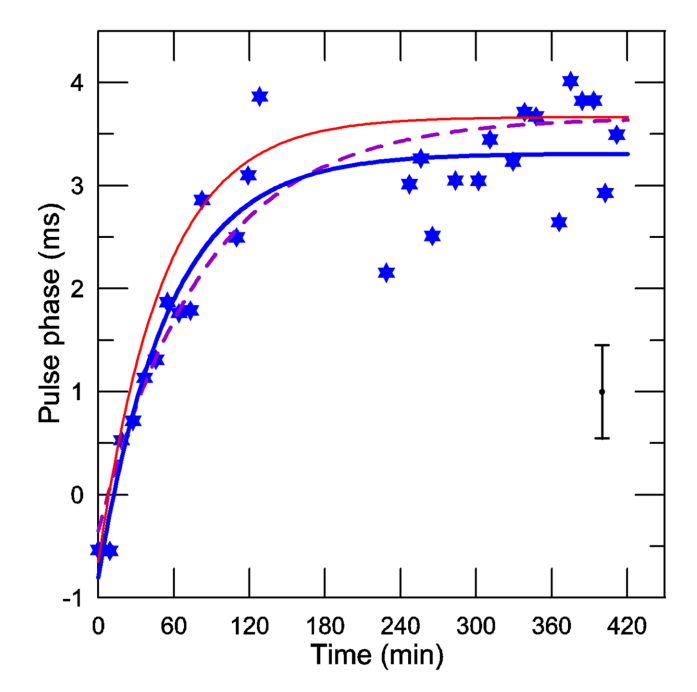


Figure 7. Corrected values of the average-profile phase are plotted as a function of time (asterisks). Each profile is obtained by integration of 500 consecutive individual pulses at 325 MHz. The standard error of phase determination is 0.45 ms. The dependence is well described by an exponential function with an amplitude of 4.1 ms and a characteristic time of 56 min (blue line). The exponential functions at low frequencies are shown for comparison. At 53.8 MHz (Bilous et al. 2014), the corresponding parameters are 4.0 ms and 84 min (dashed purple line), while at 112 MHz, the values are 4.3 ms and 51 min (thin red line). To align asymptomatic values the data at 112 MHz were shifted in the y-axis on 2.5 ms. Despite the use of different measurement methods, the results at 325 and 112 MHz coincide within their errors. In order to more clearly distinguish the corresponding lines, the 112-MHz curve has been additionally shifted by 0.4 ms.

opposite directions if a pulse delay effect exists at 327 MHz. As soon as the amplitude of the second component decreases down to 0.7, the contribution of any 'pulse delay' effect on pulse position begin to dominate. The upper panel in Fig. 6 shows the difference between the measured and simulated shift data. After subtracting the polynomial, the pulse phases pass into the range of positive values associated with the 'pulse delay' effect we are looking for. The amplitude of the change is about 1.3. It is obvious that the measurement results at 325 and 327 MHz are in good agreement with each other.

Fig. 7 shows the corrected phase values plotted against the B-mode age at 325 MHz (asterisks). This dependence is well described by an exponential function with amplitude of 4.1 ms and a characteristic change time of 56 min. For comparison, we present exponential function at low frequencies. At frequency range 25-80 MHz with a centre frequency of 53.8 MHz (Bilous et al. 2014), the corresponding parameters are 4.0 ms and 84 min. Observations at a frequency of 53.8 MHz were carried out at LOFAR in 2013 while tracking the source in its B mode for nearly 4 h. We have used the published data of three sets of observations, namely L169237, L99010, and L102418, to fit exponential function.

At a frequency of 112 MHz, our measurements exhibit an exponential change of the pulse phase with an amplitude of about 4.3 ms and characteristic time of about 51 min. Measurements were obtained by applying the timing method to several hundred profiles computed from 3.5-min transits of the pulsar through the LPA beam during the years 2008–2018. The B-mode age for each set of individual pulses was calculated from the relation assuming power-law time- $f_3$  dependence (Suleymanova & Pugachev 2017):

$$t(\min) = (f_3 / 0.439)^{1/0.0126}, \tag{2}$$

where  $f_3$  is the subpulse fluctuation frequency obtained through Fourier analysis.

To align asymptomatic values at 112 and 325 MHz, the data at 112 MHz were shifted in the *y*-axis on 2.5 ms. As a result, the exponential functions at 325 and 112 MHz coincide within their errors. One can see that despite the use of different epochs and methods of measurements the results at 325 and 327, 112, and 53.8 MHz are in good accordance.

### 4 SUMMARY AND CONCLUSIONS

Below we summarize the main results of our work.

We have analysed new sets of observations at meter wavelengths of the mode-switching pulsar B0943+10 in order to study the systematic changes in average-pulse phase during its 'Burst' mode. Observations from the Arecibo Observatory at 327 and GMRT at 325 MHz have been used. We utilized a new method for determining the correct positions of the two closely separated components of a pulse with continuous and significant changes in their relative amplitudes.

We have shown that the gradual delay in the arrival times (computed from short average profiles) during the tens of minutes following B-mode onset is also present at meter wavelengths at an amplitude of several milliseconds. Comparison with earlier results at the lower frequencies 53.8, 62, and 112 MHz show that the character of the dependence is exponential and does not depend on frequency over a wide range.

A further significant result of the analysis is that over a wide frequency range -62 to 1400~MHz – the width of B0943+10's average-profile components does not change appreciably. This is in contrast to the strong variations in the distance between them.

Our analyses have resulted in a more accurate determination of the 327-MHz integrated-profile shape as a function of B-mode age extending up to 5.7 h. For time intervals 7 to 344 min, the component-amplitude ratio gradually changes from 1.1 to 0.2 according to the more precise relation:

$$R = 0.18 + \exp(-t/73 \text{ min}),\tag{3}$$

It is interesting that at 327 MHz, the characteristic times of exponential change of both the component-amplitude ratio R and the subpulse drift rate  $f_3$  are the same. However, the evolution of the average-pulse shape with B-mode age in the range 42–327 MHz (Suleymanova & Rankin 2009) demonstrates a strong characteristic dependence on frequency. The lower the frequency, the smaller the amplitude of the R change. This behaviour contrasts with the frequency independence of the subpulse-drift and the pulse-delay properties during the bright mode. The discovery of a new frequency-independent phenomenon makes it possible to better understand the processes occurring in the magnetosphere of the PSR B0943+10.

It is reasonable to conjecture that the frequency-independent processes in the pulsar magnetosphere are closely connected to conditions in the vacuum gap near the surface of the neutron star. As it has been discussed by Bilous et al. (2014), a continuous increase in the height of the vacuum gap during the B mode results in a larger discrepancy between the star and the non-corotating magnetosphere

spin period. This is one of the possible reasons for the regular lag in the profile arrival times. If the processes displacing the profile TOAs and changing the B-mode subpulse-drift rate are associated with a smooth change in the electric potential simultaneously along and across the magnetic field lines of the magnetosphere, then the frequency independence of these phenomena finds a plausible explanation.

This result can be used to propose a scenario of the events occurring in the process of emission mode change in pulsar B0943+10. Let us first consider the correlated variations in average pulse shift and intensity. The fact that the Q-mode pulses do not undergo a shift with time, in contrast to the B mode, was shown by Bilous et al. (2014). In the article on the detection of two modes of this pulsar, it was shown that the radiation regime of the Q mode is very stable throughout its entire duration. In contrast to the average B-mode pulse, the Q-mode pulse has the form of two practically merged components with an intensity several times less than the typical intensity of an average pulse in the B mode (Suleymanova & Izvekova 1984). Later It was found that the intensity of radio emission in the B mode does not remain constant, but more than doubles with the age of the B mode (Suleymanova & Rodin 2014). It was also found that the average pulses of the B mode in the first minutes after the start have an intensity comparable to that of the

Moreover, in Q-to-B transitions, the Q-mode pulse position coincides with the initial B-mode position within errors of measurement (Bilous et al. 2014). It follows that the emission of the Q mode occurs at the minimum height of the vacuum gap. This circumstance also determines the relatively lower intensity of the Q-mode pulses. A gradual increase in the gap height entails, in our opinion, not only a displacement of the B-mode pulses but also a continuous increase in its intensity with time. At the end of this process, the gap height apparently reaches some critically large value, after which it sharply decreases, which leads to a B-to-Q transition and to a stable regime of radiation corresponding to the minimum potential value along and across the magnetic field lines.

In a while, this regime is interrupted by transition back to the B mode. It take place at the initially minimum vacuum gap height and is associated with a sudden increase in potential across the magnetic field lines, resulting in a 'carousel' beam system (Deshpande & Rankin 1999, 2001).

Our analysis shows that this process is non-monotonic. It is known that the radius of the carousel, determined by the distance between the components in the pulse profile of the B mode at a given frequency, does not change with the age of the B mode. However, there is an indication that the carousel formation process has a primary stage that lasts for several revolutions of the star and has a smaller carousel radius. This is indicated by rare episodes of the drift of subpulses that form the Q-mode shape immediately before the Q-to-B mode transition (Rankin & Suleymanova 2006).

Concerning the short primary stage in the gap condition, it is noteworthy that in the first minutes after the B-mode onset, the values of the drift rate of the subpulses, the ratio R of the average pulse and its shift with the B-mode age significantly deviate from the expected exponential behaviour. For example, according to Fig. 4 the regular change in R with time begins 7 min after the B-mode onset. The study of the processes occurring in the near vicinity of mode switching seems to be the next stage in the study of the anomalous pulsar B0943  $\pm$ 10.

From this point of view, a large contribution to the study can bring a new and thorough investigation of the average pulse shape evolution with time and frequency. A change in the potentials in the vacuum gap should cause a redistribution of the density gradients of the secondary emitting plasma, which, in turn, changes the conditions for wave propagation. The strong frequency dependence of the pulse shape evolution can be explained, in particular, with refraction effects (Barnard & Arons 1986; Lyubarskii & Petrova 1998).

It was shown earlier that the pulse shape evolution with the B-mode age at 42, 62, 112, and 327 MHz demonstrates the presence of its several stages. The first 5 min after the B-mode onset is a time when the difference in the pulse shape at far-separated frequencies is largest. These differences decrease and are minimal after another critical time of about 40 min (Suleymanova & Rankin 2009). We admit that these stages can be associated with the corresponding stages in the change of potentials in the vacuum gap of the pulsar.

### **ACKNOWLEDGEMENTS**

We are grateful to Dr. Dipanjan Mitra of the National Centre for Radio Astrophysics who kindly placed at our disposal the raw 325-MHz observations partially underlying this paper (PSR B0943+10, recorded 2010 January 14). One of us (JMR) wishes to acknowledge support from US National Science Foundation grants 09-68296 and 18-14397. The National Astronomy and Ionosphere Center (Arecibo Observatory) is operated by the University of Central Florida under a cooperative agreement with the US National Science Foundation, and in alliance with Yang Enterprises and the Ana G. Méndez-Universidad Metropolitana. This work made use of the NASA ADS astronomical data system.

#### 5 DATA AVAILABILITY

The 112- (PRAO) and 327-MHz (Arecibo) observations will be shared on a reasonable request to the corresponding author: SAS and JMR

Backus I., Mitra D., Rankin J. M., 2011, MNRAS, 418, 1736

### REFERENCES

224, 49

Barnard J. J., Arons J., 1986, ApJ, 302, 138
Bilous A. V., 2018, A&A, 616, 16
Bilous A. V. et al., 2014, A&A, 572, 14
Deshpande A. A., Rankin J. M., 1999, ApJ, 524, 1008
Deshpande A. A., Rankin J. M., 2001, MNRAS, 322, 438
Hermsen W. et al., 2013, Science, 339, 436
Lyubarskii Y. E., Petrova S. A., 1998, A&A, 333, 181
Mereghetti S. et al., 2016, ApJ, 831, 21
Phillips J. A., Wolszczan A., 1989, ApJ, 344, L69
Rankin J. M., Suleymanova S. A., 2006, A&A, 453, 679
Suleymanova S. A., Izvekova V. A., 1984, Sov. Astron., 28, 32
Suleymanova S. A., Rankin J. M., 2009, MNRAS, 396, 870
Suleymanova S. A., Rodin A. E., 2014, Astron. Rep., 58, 769
Vitkevich V. V., Alekseev Y. I., Zhuravlev V. F., Shitov Y. P., 1969, Nature,

This paper has been typeset from a TFX/LATFX file prepared by the author.